

Cite this: *Phys. Chem. Chem. Phys.*, 2011, **13**, 11045–11054

www.rsc.org/pccp

PAPER

Testing the use of molecular dynamics to simulate fluorophore motions and FRET

Evelyne Deplazes, Dylan Jayatilaka and Ben Corry*

Received 21st February 2011, Accepted 5th April 2011

DOI: 10.1039/c1cp20447e

Fluorescence resonance energy transfer (FRET) is commonly used to determine the proximity of fluorophores, but usually many assumptions are required to gain a quantitative relationship between the likelihood of energy transfer and fluorophore separation. Molecular Dynamics (MD) simulations provide one way of checking these assumptions, but before using simulations to study complex systems it is important to make sure that they can correctly model the motions of fluorophores and the likely FRET efficiency in a simple system. Here we simulate a well characterised situation of independent fluorophores in solution so that we can compare the predictions with expected values. Our simulations reproduce the experimental fluorescence anisotropy of Alexafluor488 and predict that of AlexaFluor568. At the ensemble level we are able to reproduce the expected isotropic and dynamic motion of the fluorophores as well as the FRET efficiency of the system. At the level of single donor–acceptor pairs, however, very long simulations are required to adequately sample the translational motion of the fluorophores and more surprisingly also the rotational motion. Our studies demonstrate how MD simulations can be used in more complex systems to check if the dynamic orientation averaging regime applies, if the fluorophores have isotropic orientational motion, to calculate the likely values of the orientation factor κ^2 and to determine the FRET efficiency of the system in both dynamic and static orientational averaging regimes. We also show that it is possible in some situations to create system specific relationships between FRET efficiency and fluorophore separation that can be used to interpret experimental data and find any correlations between κ^2 and separation that may influence distance measurements.

1. Introduction

Fluorescence resonance energy transfer (FRET) spectroscopy is an important tool to investigate the structure, spatial-temporal dynamics and co-localisation of proteins and other biomolecular systems. FRET is a dipole–dipole, non-radiative energy transfer from an electronically excited ‘donor’ fluorophore to a suitable ‘acceptor’ fluorophore. The technique is based on the finding that the likelihood of the energy transfer (known as FRET efficiency) is dependent on the fluorophore separation.^{1,2} If the fluorophores are attached to known sites within a molecule or parts of a cell, FRET efficiency can be used to determine the proximity of the probes and potentially as a measure of inter and intramolecular distances in the range of 10–100 Å.² FRET has been widely employed to study a large range of systems^{3–6} and more recently extended to single-molecule measurements.^{7–9}

The recent popularity of FRET has given rise to a series of studies that re-examine the validity of using FRET for

quantitative distance measurements. One aspect that complicates the experimental verification, such as carried out in the original experiment by Stryer and Haugland,² is that the presumably fixed distances between fluorophores might not be as well defined as expected. Schuler *et al.*⁹ and Best *et al.*¹⁰ revisited the Stryer and Haugland experiment and showed that deviations of FRET efficiencies from expected values were due to the previously unmeasured flexibility of the linkers causing a deviation of the donor–acceptor separation from the assumed fixed value. Alternatively, the use of FRET for quantitative distance measurements may be complicated if any of the assumptions underlying the theory or the experiment break down (discussed in detail below). A number of recent studies employed Molecular Dynamics (MD) simulations to investigate these assumptions and their effect on FRET experiments.^{11–15} The results indicated that some of the assumptions may break down under certain conditions and depend on the specific environment of the fluorophores. The results suggest that it is important to carefully consider the effect of these assumptions when designing FRET experiments for a specific system.

Clearly MD simulations can provide valuable insight into the behaviour of fluorophores at the molecular level and their

School of Biomedical, Biomolecular and Chemical Sciences,
The University of Western Australia, Perth, Australia.
E-mail: ben.corry@uwa.edu.au

effect on the assumptions commonly made in FRET experiments. As such, simulations can be helpful in designing and analysing FRET experiments. However, before using simulations to study complex systems it is important to ensure that MD is capable of correctly describing the rotational and translational motion of the fluorophores which are crucial for modeling FRET. The best way to validate the use of MD simulations for understanding FRET is to study a simple model system where the expected values are known. This paper reports such a study by examining the rotational and translational motion, and FRET efficiency of a system of independent fluorophores in solution. Although this situation does not directly replicate the type of biological systems most commonly investigated by FRET, a simple model provides the important advantage of knowing the expected results (fluorophores should have unrestricted rotational and translational motion). These simulations can also be used to obtain system specific relationships between FRET efficiency and fluorophore separation and to derive protocols for testing the accuracy of the assumptions inherent in the experiment. These generic protocols can then be applied to MD simulations of more complex systems.

2. Theory

Since Stryer and Haugland originally labeled FRET a “spectroscopic ruler”,² the validity of employing FRET for quantitative distance measurements has been widely debated. The controversy stems from several assumptions that are either inherent to the Förster theory or are commonly made in FRET experiments. The first assumption is that the lateral diffusion of the fluorophores is much slower than their rotational motion such that the energy transfer takes place at constant fluorophore separation. Secondly, the ideal dipole approximation (IDA) assumes that the coupling between the donor and acceptor can be described by dipole–dipole interactions. These two assumptions are inherent to the Förster theory.

Further assumptions commonly made in FRET experiments relate to how the FRET efficiency is calculated when averaging over time and ensembles of donors and acceptors. The FRET efficiency (E) for a single donor–acceptor (DA) pair depends on the fluorophore separation R and the relative orientation of the donor and the acceptor, quantified by the orientation factor κ^2 , both of which may vary in time, and a constant c :¹⁶

$$E = \frac{c\kappa^2}{R^6 + c\kappa^2} \quad (1)$$

The third assumption relates to whether it is possible to use an average value of κ^2 in eqn (1). If the rotational motion of the fluorophores is much faster than the energy transfer rate the fluorophores visit all possible orientations during the transfer event and the time-averaged value of κ^2 ($\langle\kappa^2\rangle$) can be used. This case is referred to as the dynamic orientational averaging regime and the time averaged FRET efficiency is given by

$$E_{\text{dynamic}} = \left\langle \frac{c\langle\kappa^2\rangle}{R(t)^6 + c\langle\kappa^2\rangle} \right\rangle \quad (2)$$

In contrast, the static orientational averaging regime applies if the rate of re-orientation is small compared to the transfer rate.

In this case the instantaneous value of κ^2 at the time of transfer is used:

$$E_{\text{static}} = \left\langle \frac{c\kappa^2(t)}{R(t)^6 + c\kappa^2(t)} \right\rangle \quad (3)$$

The inability to experimentally measure the instantaneous value of κ^2 has led Dale and Eisinger¹⁶ to note that ‘the static limit, therefore, does not readily lend itself to intramolecular distance determinations...’.

It is possible that values of κ^2 and R are not independent, for example if the fluorophores directly interact or are joined by a stiff linker.¹⁴ The use of eqn (2) implicitly assumes that κ^2 and R are independent variables such that $\langle\kappa^2\rangle\langle R\rangle = \langle\kappa^2R\rangle$. If κ^2 and R are correlated then a different value of $\langle\kappa^2\rangle$ is required for each fluorophore separation R . The fourth commonly used assumption is that there is no such correlation meaning a single value of $\langle\kappa^2\rangle$ relates E and R .

The fifth assumption relates to the specific value of $\langle\kappa^2\rangle$ (and thus is only relevant in the dynamic regime) and depends on the rotational freedom of the dyes. If the fluorophores exhibit unrestricted rotational motion such that they sample the full range of orientations with equal probability, the so-called isotropic condition is fulfilled and $\langle\kappa^2\rangle = 2/3$. This approximation is usually safe for systems of independent fluorophores in solution or when they are attached to small and flexible molecules. Attaching the dyes to large or rigid host systems can limit their rotational freedom such that the requirements for the isotropic condition are no longer met.^{13,15,17} Hence even if the dynamic condition is fulfilled and $\langle\kappa^2\rangle$ can be used, its numerical value need not be $2/3$.

Finally, in many experiments multiple donors and acceptors are present. As described in Methods section, this changes the FRET efficiency and the expression describing that a single DA pair (eqn (1)) must be replaced by one involving multiple pairs.

In theory the dynamic and isotropic conditions are independent assumptions, although in practice both are usually assumed to be true. In order to exploit the quantitative relationship between measured FRET efficiency and donor–acceptor separation the numerical value of κ^2 needs to be known. Since it is not possible to experimentally determine instantaneous values of $\kappa^2(t)$ it is necessary to assume that the dynamic condition is fulfilled such that $\langle\kappa^2\rangle$ can be employed. Yet even this value is hard to measure experimentally^{16,18} and consequently most FRET experiments assume that the isotropic condition is true such that $\langle\kappa^2\rangle = 2/3$ and the R^{-6} relationship between E and R holds (eqn (2)).

The validity of these assumptions and their limiting effect on using FRET for quantitative distance measurements have been discussed widely over the past 5 decades.^{14,16,19–22} The numerical value of κ^2 has been described “at best a nuisance and at worst an insurmountable problem”.²¹ Dale and Eisinger^{16,19,20} were among the first to critically investigate the $\langle\kappa^2\rangle = 2/3$ approximation and showed that even if the exact value of $\langle\kappa^2\rangle$ cannot be determined it need not pose an insurmountable problem. They developed a theoretical model¹⁹ and an experimental procedure¹⁶ to determine limits of $\langle\kappa^2\rangle$ from the donor and acceptor emission anisotropy

under dynamic conditions. $\langle \kappa^2 \rangle_{\min}$ and $\langle \kappa^2 \rangle_{\max}$ enable the calculation of a possible range of R and thus provide an estimate on the error introduced by assuming $\langle \kappa^2 \rangle = 2/3$. More recently, Corry *et al.*¹⁸ reported a method that uses fluorescence intensity from confocal microscope images to determine the mean orientation and distribution of membrane-bound fluorophores and thus put limits on the range of $\langle \kappa^2 \rangle$ values. Ivanov *et al.*²³ reported a method for using emission anisotropy measurements to estimate the error in FRET distance measurements due to the unknown value of $\langle \kappa^2 \rangle$.

3. Methods

3.1 MD simulations

The simulation system consisted of 8 Alexafluor488 (AF488, donor) and 8 Alexafluor 568 (AF568, acceptor) molecules in a cubic box with side lengths of 200 Å corresponding to a total dye concentration of 3.32 mM. The Alexafluor molecules are depicted in Fig. 1. The system was solvated with TIP3 water and neutrality was retained by adding sodium and chloride ions, bringing the total count of atoms to 781 533. Such a large system was used to avoid dependence of the results on periodic cell size. The simulation was carried out with the NAMD software package²⁴ using the previously obtained structures and parameters for the dyes¹⁵ and the CHARMM27 all atom force field^{25,26} for water and ions. Bond lengths to H atoms were kept fixed as a 2 fs time step was used. The electrostatic interactions were calculated using the particle-mesh Ewald scheme and the Lennard-Jones interactions were calculated with a 1.2 nm cut-off. Langevin dynamics was used to control the temperature with a damping coefficient of 5 ps⁻¹ and was applied to all atoms except hydrogen. The simulation was performed at constant temperature (298 K) and pressure (1 atm) with periodic boundary conditions for a total of 30 ns.

3.2 Data analysis

The direction of the unit vectors for the transition dipole moments of the donor (\hat{d}) and acceptor (\hat{a}) molecules was taken along the long axis of the outer rings in the head groups (Fig. 1) as determined in previous *ab initio* calculations.¹⁵ The distance between the donor and acceptor dye is defined by

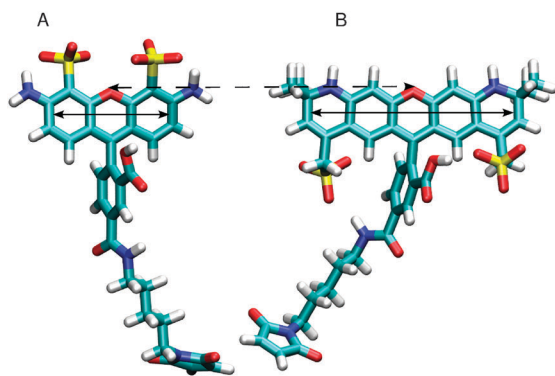


Fig. 1 Structures of AlexaFluor dyes AF488 (A) and AF568 (B). The direction of the transition moments (solid lines) is indicated by the arrows. The vector connecting the dyes (dashed line) defines the fluorophore separation.

the connection vector \hat{r} that joins the central oxygen in the head group of the dyes as shown in Fig. 1. All data in the analysis are calculated using the values of \hat{d} , \hat{a} and \hat{r} at every time step, extracted from the trajectories. The simulation was performed using periodic boundary conditions but the data analysis was performed considering the following DA pairs. For the analysis of κ^2 only the 8 donors and 8 acceptors (64 DA pairs) in the central box of the simulation were used (*i.e.* not including the images created by the periodic boundary conditions). Since each copy of a fluorophore in the central box will have the same transition dipole, considering periodic images will not add independent values of κ^2 to the data set. The same 64 DA pairs were used for the analysis of the translational diffusion of the fluorophores and the distribution of fluorophore separation was compared to an expected distribution corresponding to the same situation, calculated using randomly generated fluorophore coordinates in a box of the same size as the simulation system. The FRET efficiency was calculated by including the donors and acceptors in the central box and adding the acceptors in all 26 surrounding boxes created by the periodic boundary conditions (8 donors and 8×27 acceptors giving a total of 1728 DA pairs). This ensures that each donor is surrounded by a bulk solution of acceptors up to a range greater than $2R_0$.

The time-resolved decay of fluorescence anisotropy for each donor and acceptor was calculated using an approach similar to that described in ref. 17. Assuming an ensemble of fluorophores with random isotropic initial orientations, the fluorescence anisotropy of an individual fluorophore can be calculated by

$$r(t) = \frac{2}{5} \langle P_2[\mu(0)\mu(t)] \rangle \quad (4)$$

where $P_2(x) = (3x^2 - 1)/2$, $\mu(0)$ and $\mu(t)$ are the transition dipole moments (\hat{d} , \hat{a}) at time of excitation (0) and at some time later (t). The time-average, represented by the angle brackets, was calculated by assigning each frame in the simulation to $t = 0$ and calculating the mean of the resulting $r(t)$ for a series of subsequent times $0 + t$. The rotational correlation time (τ_θ) was determined by fitting the final $r(t)$ to a single exponential:

$$r(t) = r_0 e^{-t/\tau_\theta} \quad (5)$$

where r_0 is the fundamental anisotropy of the dye observed in the absence of other depolarizing processes such as rotational diffusion or energy transfer.

The orientation factor κ^2 was calculated for each DA pair at each frame using

$$\kappa^2 = (\cos \theta_T - 3 \cos \theta_D \cos \theta_A)^2 \quad (6)$$

where θ_T is the angle formed by \hat{d} and \hat{a} , θ_D (θ_A) is the angle between \hat{d} (\hat{a}) and \hat{r} . Under isotropic conditions when all possible orientations of \hat{d} and \hat{a} are equally probable, the frequency distribution of κ^2 is given by²²

$$\rho(\kappa^2) = \begin{cases} \frac{1}{2\sqrt{3}\kappa^2} \ln(2 + \sqrt{3}) & 0 \leq \kappa^2 \leq 1 \\ \frac{1}{2\sqrt{3}\kappa^2} \ln\left(\frac{2+\sqrt{3}}{\sqrt{\kappa^2+\sqrt{\kappa^2-1}}}\right) & 1 \leq \kappa^2 \leq 4 \end{cases} \quad (7)$$

Histograms of $\rho(\kappa^2)$ vs. κ^2 were determined for each individual DA pair and for the overall system. Average κ^2 values were calculated from the $\rho(\kappa^2)$ vs. κ^2 curves as well as by averaging the instantaneous κ^2 values. Uncertainties for the latter were determined from standard deviations.

For the remainder of this paper we use the following symbols to distinguish between the different averages of κ^2 : (i) $\kappa_{ij}^2(t)$ refers to the instantaneous value of κ^2 for a specific DA pair ij at time t , (ii) $\langle \kappa_{ij}^2 \rangle$ is the time-averaged κ^2 for DA pair ij and (iii) $\langle \kappa^2 \rangle$ is a system wide average obtained from averaging $\langle \kappa_{ij}^2 \rangle$ over all DA pairs.

The autocorrelation of κ_{ij}^2 ($C_{ij}(t)$) for each DA pair was used as a measure of orientational averaging and calculated by

$$C_{ij}(t) = (\langle \kappa_{ij}^2(0) \rangle - \langle \kappa_{ij}^2 \rangle)(\kappa_{ij}^2(t) - \langle \kappa_{ij}^2 \rangle) \quad (8)$$

The time average was obtained analogously to that for the anisotropy decay. A system wide average, $C(t)$, was calculated by averaging the $C_{ij}(t)$ curves of all DA pairs. The time constant τ_{κ^2} was determined by fitting the time-resolved decay of $C(t)$ to a single exponential.

$$C(t) = C_0 e^{-t/\tau_{\kappa^2}} \quad (9)$$

Oriental averaging of the donor and the acceptor is complete when $C(t)$ reaches zero.

For a single DA pair, separated by distance R , the efficiency of energy transfer (E) is given by

$$E = \frac{R_0^6}{R_0^6 + R^6} = \frac{\frac{R_0^6}{R^6}}{1 + \frac{R_0^6}{R^6}} \quad (10)$$

where R_0 is the so-called Förster distance at which E is 50%. R_0 is defined by the spectral properties of the dyes, the medium in which the experiment is carried out and the value of κ^2 . Hence R_0 can be expressed as $R_0^6 = c\kappa^2$. R_0 is reported as 62 Å for the fluorophores used in this simulation assuming $\kappa^2 = 2/3$.²⁷

In systems with multiple donors and acceptors the relationship between E and R can no longer be described by eqn (10) but needs to account for the energy transfer between each donor and every acceptor. In this case E was calculated for both static and dynamic conditions for each time t in the simulation using

$$E_{\text{static}}(t) = \frac{1}{m} \sum_{i=1}^m \frac{\sum_{j=1}^n \frac{c\kappa_{ij}^2(t)}{R_{ij}^6(t)}}{1 + \sum_{j=1}^n \frac{c\kappa_{ij}^2(t)}{R_{ij}^6(t)}} \quad (11)$$

$$E_{\text{dynamic}, \langle \kappa^2 \rangle \langle R \rangle}(t) = \frac{1}{m} \sum_{i=1}^m \frac{c \langle \kappa^2 \rangle \sum_{j=1}^n \frac{1}{R_{ij}^6(t)}}{1 + c \langle \kappa^2 \rangle \sum_{j=1}^n \frac{1}{R_{ij}^6(t)}} \quad (12)$$

where m and n are the total number of donors and acceptors and i and j refer to specific donors and acceptors. Eqn (11) is used to calculate the FRET efficiency for a system of fluorophores of statically averaged orientations as it does

not relate FRET efficiency and R with a system wide average $\langle \kappa^2 \rangle$ but considers the relative orientation of every DA pair ij at time t . If the dynamic condition is fulfilled $\kappa_{ij}^2(t)$ can be replaced by $\langle \kappa^2 \rangle$ implying $\langle \kappa^2 \rangle \langle R \rangle = \langle \kappa^2 R \rangle$ (eqn (12)).

E was calculated for each frame in the simulation and used to obtain the frequency distributions of E which was subsequently used to calculate the average FRET efficiency (\bar{E}). We did not consider the possibility of homo-FRET in our analysis.

The energy transfer time (τ_T), given by the inverse of the transfer rate (k_T), was calculated by

$$\frac{1}{\tau_T} = k_T = \frac{1}{\tau_D} \left(\frac{R_0}{R} \right)^6 \quad (13)$$

where τ_D is the lifetime of the donor in the absence of the acceptor. Comparing τ_{κ^2} and τ_T determines which averaging regime applies. If $\tau_{\kappa^2} \ll \tau_T$ the re-orientation of the dyes is much faster than the time taken for the energy transfer. In this case the dynamic condition is fulfilled. On the other hand, if $\tau_{\kappa^2} \gg \tau_T$ the static averaging regime applies. If τ_T is not known, τ_D may be used as an approximation in its place given that it will typically be of a similar order of magnitude but a little larger. We note that these comparisons are only helpful when τ_T is either much greater or much lesser than τ_{κ^2} .

4. Results and discussion

4.1 Fluorescence anisotropy decay

It is important to verify the MD model to ensure that the force fields used to describe the individual dyes are well parameterized and the setup and parameters of the simulation are reasonable. One way of achieving this is to compare the fluorescence anisotropy calculated from the simulation data to the experimental value. Fig. 2 shows the anisotropy decay of all

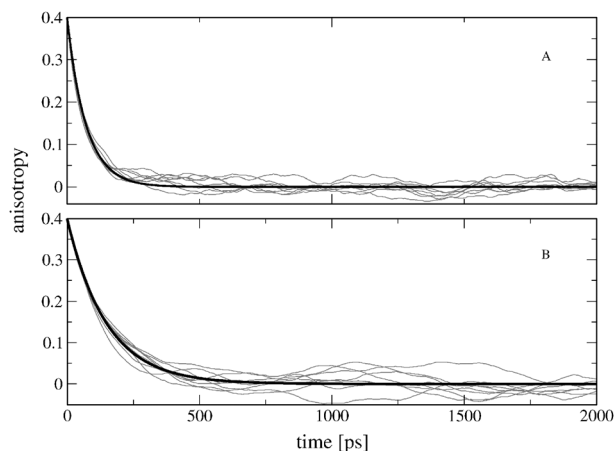


Fig. 2 Calculated fluorescence anisotropy decay for all AF488 (A) and AF568 (B) dyes (grey lines) and their averages (black lines). The average decay for AF488 is indistinguishable from the decay calculated from the experimental rotational correlation time.

AF488 and AF568 molecules in the system that was used to calculate their average rotational correlation time (τ_θ). We did not find any experimental value of τ_θ for AF568. The data show consistent behaviour for all dyes of the same type. The average τ_θ for AF488 was calculated to be 143 ps, consistent with the experimental value of 170 ps. The rotational correlation time of AF568 is larger but of the same magnitude as the value for the AF488. As the AF568 has a larger head group it can be expected to show slower rotational diffusion.

4.2 Simulations of κ^2

To assess whether FRET is occurring in a dynamic or static averaging regime we plot the autocorrelation decay of κ^2 (Fig. 3). The fitted value of τ_{κ^2} was calculated to be 25 ps (eqn (9)). The fluorescence lifetime of the donor (τ_D) is reported by the manufacturer as 3.6 ns. Hence there are molecular motions which are much faster than the transfer time, which would suggest that the system is in a dynamic regime. However, this is not the case as $C(t)$ does not decay to zero at long time intervals but goes below zero at about 200 ps. This probably means that there are slower molecular motions associated with the autocorrelation curve. This would not be unusual and multi-exponential time decays are commonly used in experimental analysis of fluorescence anisotropy.²⁸ In this model system the dyes in solution should be dynamic and isotropic. The only question is whether the MD simulation has been performed for long enough to capture this.

The benefit of using a simple model system is that we know the expected average value and probability distribution of isotropic $\langle \kappa^2 \rangle$. Fig. 4 and 5 tests whether the simulation reproduces these expectations.

Fig. 4 shows plots of $\kappa_{ij}^2(t)$ and its cumulative average vs. time for four DA pairs. The data show that $\kappa_{ij}^2(t)$ covers the full range from 0 to 4 indicating that the fluorophores do visit all possible relative orientations. Analysis of all cumulative averages shows that they converge to a stable value after ~ 16 ns of simulation, but there are oscillations long after 25 ps. These results also support that there are longer-time

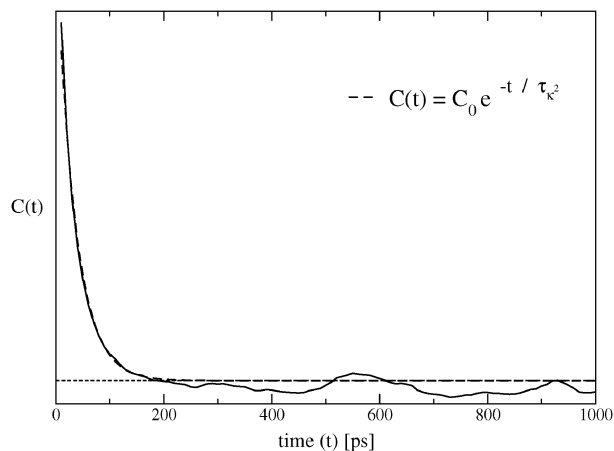


Fig. 3 Autocorrelation decay of κ^2 ($C(t)$) (solid line). τ_{κ^2} (25 ps) was obtained by fitting $C(t)$ to a single exponential (dashed line) using eqn (9).

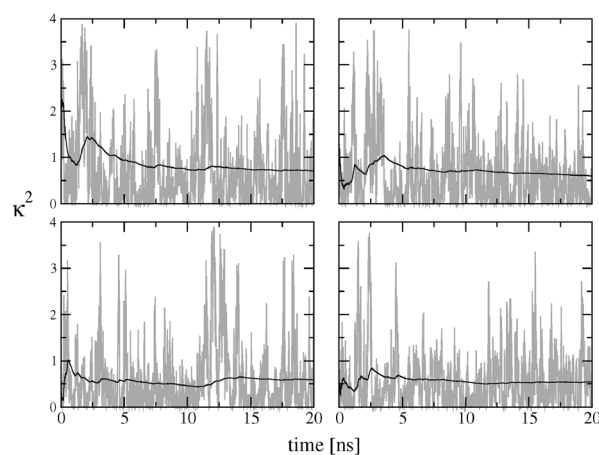


Fig. 4 Time-dependent fluctuations of the orientation factor $\kappa_{ij}^2(t)$ for selected DA pairs for the first 20 ns of simulation. Instantaneous values (grey lines) and cumulative averages (black lines) are shown.

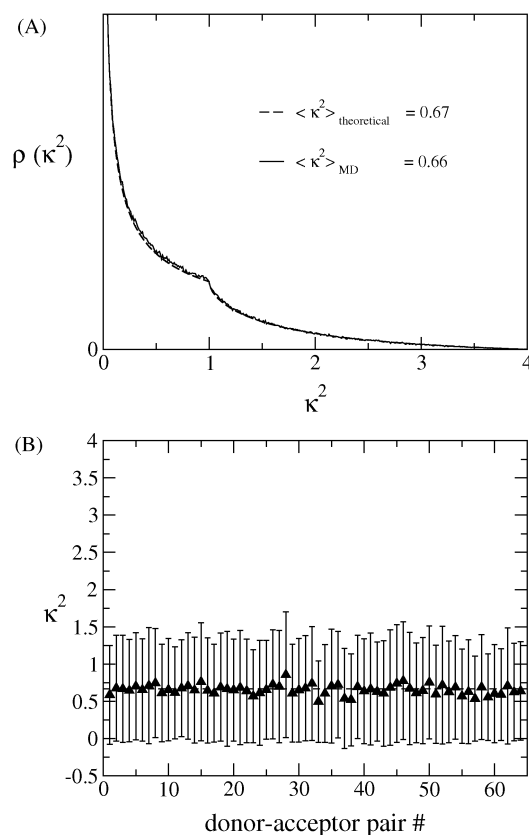


Fig. 5 (A) Frequency distribution of κ^2 (dashed line) calculated from the simulation data in comparison to the theoretical distribution (solid line). (B) $\langle \kappa_{ij}^2 \rangle$ values and standard deviations for all 64 DA pairs in the central box of the simulation system. The average over all DA pairs ($\langle \kappa^2 \rangle$, dashed line) is 0.66 ± 0.06 .

rotational motions, but the fact that the cumulative average settles after 16 ns suggests that all rotational motions are well sampled within the 30 ns of simulation.

The frequency distribution of κ^2 obtained from all DA pairs (Fig. 5A) is used as another check that the isotropic condition is met. The distribution from the simulation data shows very

good agreement with the theoretical distribution. $\langle \kappa^2 \rangle$ is 0.66 ± 0.06 ; a close agreement with the expected $2/3$. This suggests that the model reproduces the isotropic condition on an ensemble level.

When analysing the results on the level of individual DA pairs the data paint a different picture. Fig. 5B reports $\langle \kappa_{ij}^2 \rangle$ for each DA pair. Despite the close agreement of $\langle \kappa^2 \rangle$ to $2/3$, $\langle \kappa_{ij}^2 \rangle$ values range from 0.49 to 0.87 and show very large standard deviations as indicated by the error bars. There are two possible explanations for the large deviations. Firstly, the fact that all values are well within the error bars of $2/3$ suggests that the variation of $\langle \kappa_{ij}^2 \rangle$ for each pair may represent normal fluctuations and noise in the data. In this case $\langle \kappa_{ij}^2 \rangle$ values would approach $2/3$ if the simulation time is increased. Secondly, the discrepancy between $\langle \kappa_{ij}^2 \rangle$ and $2/3$ may also be an indication that the isotropic condition is not met for individual DA pairs. This could indicate a problem with how the rotational motion is modeled as we know that the isotropic condition should be fulfilled for independent fluorophores in solution.

To further investigate these questions we analysed the frequency distributions of the absolute orientations of individual dyes as well as their relative orientations to examine if they are undergoing isotropic motion. If the motion of each individual dye is isotropic all orientations are equally probable and, accounting for the geometric factor, the frequency distribution relative to an arbitrary axis should follow a sine curve. Fig. 6 shows the normalised frequency distributions of the orientations of the donor (θ_D) and acceptor (θ_A) transition moments as well as the angle formed by their relative orientations (θ_T) for two DA pairs; one for which $\langle \kappa_{ij}^2 \rangle = 2/3$ and one for which $\langle \kappa_{ij}^2 \rangle$ strongly deviates from $2/3$ ($\langle \kappa_{ij}^2 \rangle = 0.49$). The results clearly indicate that for the second pair both the orientations of the individual dyes and their relative orientations do not match the expected sine curve. The reason for the non-uniform distribution can either be inherent to the model or caused by insufficient sampling. We investigated the pairs with large deviations with respect to a potentially correlated motion. We found this to be unlikely as the donor and acceptor dyes are at least 25 \AA apart thus making correlated motion based on physical interactions unlikely. But a comparison of a series of frequency distributions of θ_T for pairs with $\langle \kappa_{ij}^2 \rangle$ deviating from $2/3$ at different simulation times showed that the agreement between the simulation data and the sine curve improves with increasing simulation time. This suggests that the motion of the individual DA pairs is isotropic but not sufficiently sampled causing the deviations of $\langle \kappa_{ij}^2 \rangle$. This was initially a surprising result given the time frame for the decay of $C(t)$, but is consistent with the oscillations seen in $C(t)$ and the cumulative average of κ_{ij}^2 .

It seems to take a long time to get a truly uniform distribution of the relative orientations of the dyes. We can get an order of magnitude estimate of how long by noting that the variance in $\langle \kappa_{ij}^2 \rangle$ based on N independent trials goes as $N^{-1/2}$. If we want to achieve a 1% accuracy in this quantity we would need $N \approx 10\,000$ (since then $N^{1/2}/N \approx 1\%$). To ensure that the trials are independent we should sample after a period greater than τ_{κ^2} . Thus the time required would be greater than $10\,000 \times 25 \text{ ps} = 250 \text{ ns}$.

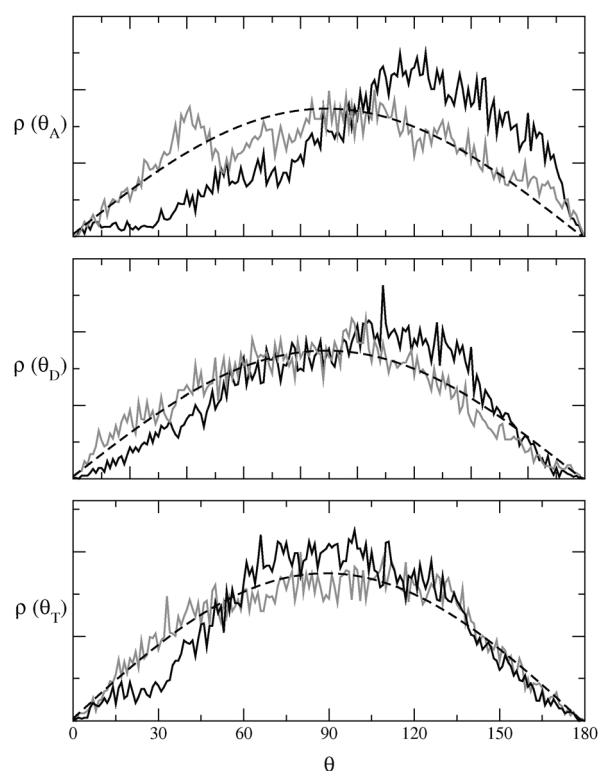


Fig. 6 Frequency distributions of donor and acceptor orientations. θ_A (θ_D) is the angle between the acceptor (donor) transition dipole moment and a primary axis of the simulation box. θ_T is the angle formed by the donor and acceptor transition dipole moments. Orientations from a DA pair with a $\langle \kappa_{ij}^2 \rangle$ close to $2/3$ (solid grey lines) and from a pair with a value that deviates from $2/3$ (solid black lines) are shown in comparison to the theoretical distribution (dashed black lines).

To further investigate this we combined the κ^2 data from the 64 DA-pairs such that they represent a data set of κ^2 values from a much longer simulation of a single DA-pair. To ensure statistically reliable results we joined the data from the DA-pairs in 500 randomly generated combinations. Analysis of the cumulative average of the combined κ^2 data indicates that on average simulations of 25 ns, 67 ns and 206 ns are required to achieve a tolerance of 10%, 5% and 1% respectively. This is consistent with the previous estimate based on the variance of $\langle \kappa^2 \rangle$ and with the fact that a 30 ns simulation predicted a $\langle \kappa^2 \rangle$ of $0.66 \pm 9\%$. Thus, 30 ns is indeed inadequate to get errors of less than 1% for each individual DA-pair. Rather than simulating a single DA-pair for longer time, in this case, reliable values were obtained by including multiple DA-pairs in the one simulation. This study presents a warning that it can take very long simulations to get reliable average of κ^2 if only a single DA-pair is included in the simulation.

4.3 Translational diffusion of fluorophores

Fig. 7A shows the donor–acceptor separation as a function of simulation time for four selected DA pairs. Compared to the results in Fig. 4, it is evident that the translational motion shows slower time dependent fluctuation than the rotational motion.

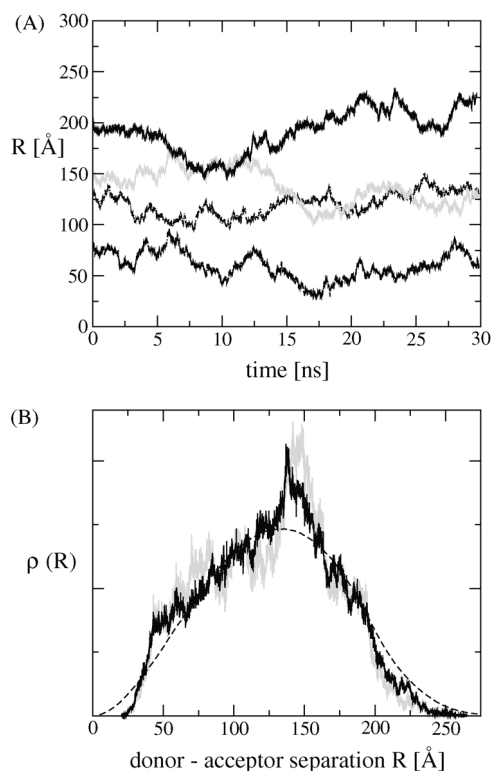


Fig. 7 (A) Donor–acceptor separation (R) vs. time for selected DA pairs over the full simulation time. (B) Frequency distribution of donor–acceptor separation (R) calculated using all 64 DA pairs in the central box. Results after 16 ns (grey line) and 30 ns (black line) are shown in comparison to the expected distribution (dashed line).

The frequency distribution of R over all DA pairs after 16 ns and 30 ns of simulation is shown in Fig. 7B. The simulation data are not compared to a distribution expected in a real bulk solution but to ‘a solution in a box’. In a real bulk solution, the probability density of finding an acceptor within a given distance R would be proportional to the spherical volume surrounding that donor (R^3). The comparison intends to test if the fluorophores have moved around enough during the 30 ns of simulation to sufficiently sample all fluorophore separations. The distribution after 16 ns of simulation strongly deviates from the theoretical curve. With increasing simulation time the sampling of R improves and approaches the expected distribution yet it still shows deviations after 30 ns. This suggests that the translational motion is not sufficiently sampled in 30 ns, but as shown below this time is long enough to gain the desired information about the distance dependence of κ^2 and FRET efficiency.

4.4 Correlation of κ^2 and R

Previous studies have shown that it is not always valid to assume that κ^2 and R are independent and their correlation can affect the calculated FRET efficiency.¹⁴ If κ^2 and R are correlated it is not possible to use eqn (12) even if the dynamic condition is fulfilled. In our simple model system, the fluorophores show fast and unrestricted rotational motions and are separated by at least ~ 25 Å, the latter being caused by the missing data of small fluorophore separations caused by

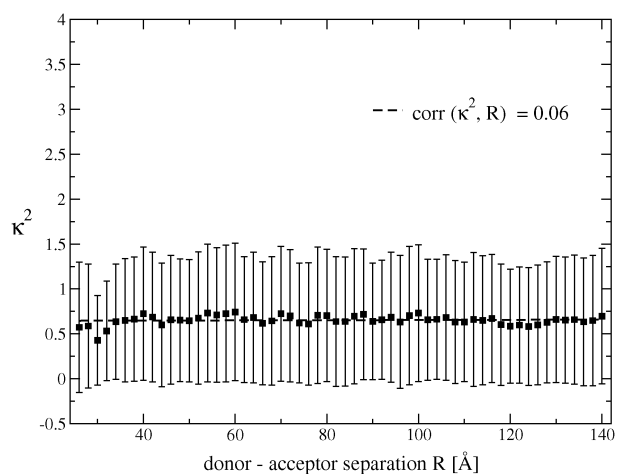


Fig. 8 Binned scatter plot of $\langle \kappa^2 \rangle$ vs. R for fluorophore separations (R) between 20 Å and 140 Å. The data over the full range of R show a very low correlation of 0.06 (dashed black line). The standard deviation of each DA pair is shown as error bars. Data below 20 Å are not shown due to under sampling of R while data above 140 Å do not affect the FRET efficiency.

insufficient sampling. This makes it unlikely for the donors and acceptors to exhibit any long range interactions that cause correlation of κ^2 and R . Fig. 8 shows a binned scatter plot of κ^2 vs. R based on $\kappa_{ij}^2(t)$ of all DA pairs over 30 ns of simulation. Only distances in the range of $25 \text{ Å} \leq R \leq 140 \text{ Å}$ are used. Distances below 25 Å are under sampled while distances above $2R_0$ are not likely to influence FRET. Despite some fluctuations, κ^2 and R show only a low positive correlation (0.06) over the analysed range of R .

4.5 Simulation of FRET efficiencies

Fig. 9 shows the frequency distributions of E_{static} and E_{dynamic} calculated from the simulation data in comparison to the corresponding theoretical distribution. The theoretical graph

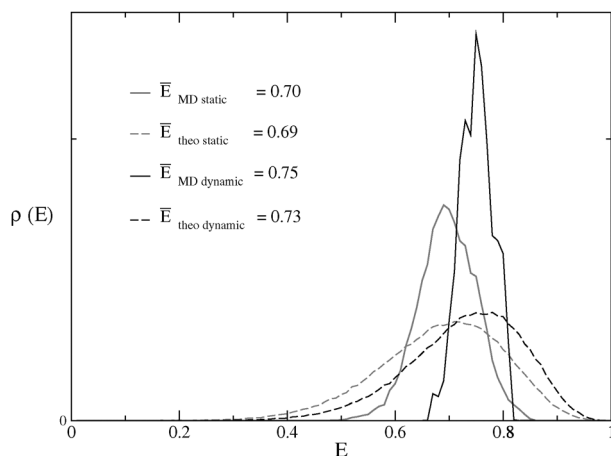


Fig. 9 Frequency distributions of FRET efficiency calculated from the simulation data for dynamic (black solid line) and static conditions (grey solid line) in comparison to the theoretical distributions (black dashed line for dynamic conditions, grey dashed line for static conditions). The time-averaged, system wide FRET efficiencies (\bar{E}) were calculated from the corresponding frequency distribution.

for the static case was prepared by calculating E (eqn (11)) using randomly generated fluorophore coordinates from a uniform distribution and κ^2 according to their theoretical frequency distributions. For the theoretical dynamic case only randomly generated fluorophore coordinates were used and E was calculated using eqn (12) with $\langle \kappa^2 \rangle = 2/3$. For both the dynamic and static case the frequency distributions calculated from the simulation data show poor agreement with the theoretical data as low and high FRET efficiencies are significantly underestimated. We explain this result as follows. In a system of multiple donors and acceptors high FRET efficiencies correspond to situations where a donor is surrounded by several acceptors at close range while low FRET efficiencies are a result of a donor with few or no acceptors within the FRET range. This indicates that these situations are poorly sampled in the simulation. Averaged FRET efficiencies (\bar{E}) were calculated for both static and dynamic conditions and the results agree well with the theoretical values despite the discrepancies in the frequency distributions.

If the experimentally observed FRET efficiency is to be used for quantitative distance measurements, the plot of FRET efficiency vs. donor-acceptor separation is crucial for data analysis. Fig. 10 shows plots of E vs. R calculated using eqn (11) and (12), for the dynamic and static case, respectively. The system wide FRET efficiencies for each frame in the simulation were binned into R -bins of 0.1 Å resolution. The theoretical graphs were prepared using the same approach as for the frequency distributions of E described previously. Under the dynamic condition the simulation data are also compared to the commonly used R^{-6} relationship. For the dynamic conditions the two graphs are not distinguishable. For the static conditions the data from the simulation show small local deviations but match the general relationship described by the theoretical graph. The results confirm that the simulation reproduces the R^{-6} relationship predicted by the Förster theory under dynamic conditions. Importantly, the

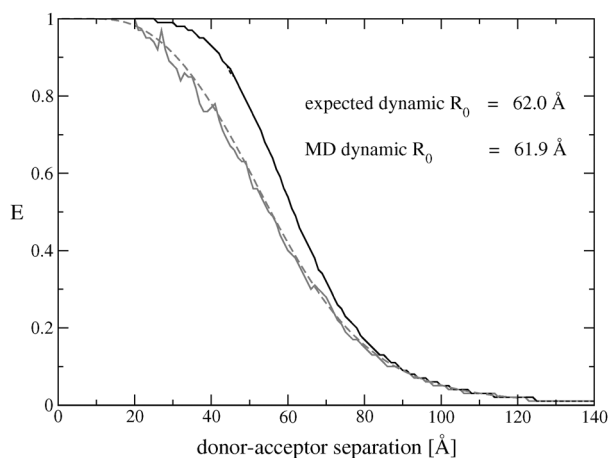


Fig. 10 FRET efficiency (E) vs. donor-acceptor separation (R) calculated from the simulation data for dynamic (black solid line) and static (grey solid line) conditions in comparison to theoretical data (black dashed line for dynamic conditions, grey dashed line for static conditions). The graphs for the dynamic conditions are indistinguishable.

under sampling of R does not seem to affect the accuracy of the calculated FRET efficiency. For statically averaged orientations the simulation also reproduces the predicted relationship.

We conclude that although the frequency distributions of E are quite poor the E vs. R curves are acceptable. This means that the simulation data can be used to predict the FRET efficiencies for a given fluorophore separation. Both static curves, theoretical and MD simulation, are very similar to results for 'slow rotating' fluorophores in Fig. 8 of Ivanov *et al.*²³ These authors obtained their figures by averaging the single-donor-acceptor expression (1) over uniform distributions of donor and acceptor orientations for fixed R . Strictly speaking an expression that considers multiple donors and acceptors should be used. In addition our results include some estimate of realistic translational diffusion of fluorophores in water.

4.6 Applications of data from FRET simulations

The following section aims to demonstrate more generally how simulations can be used to (i) test the assumptions often used in FRET experiments for a specific system of interest and (ii) derive system specific relationships between FRET efficiency and fluorophore separation for the analysis of experimental data. The approach outlined below is not specific to our model system but is applicable to FRET simulations of more complex systems.

The autocorrelation decay of κ^2 (eqn (8)) can be used to determine if the dynamic or static averaging regime applies. Using τ_D as an estimate of τ_T , then if $\tau_{\kappa^2} \ll \tau_D$ the dynamic condition is fulfilled but if $\tau_{\kappa^2} \gg \tau_D$ the static averaging regime applies. If τ_{κ^2} is of similar magnitude to τ_D it is difficult to assess which averaging regime applies.

It is also advisable to consider if $C(t)$ decays to zero. The frequency distribution of κ^2 can be used to test if the isotropic condition is fulfilled, either at an ensemble level or at the level of an individual DA pair. Alternatively, frequency distributions of the angles formed by donor and acceptor transition dipole moments (Fig. 6) can be used to test if all orientations are equally likely. Averaging values of $\langle \kappa_{ij}^2 \rangle$ over all DA pairs and simulation time give a numerical value for $\langle \kappa^2 \rangle$ to verify the $\kappa^2 = 2/3$ approximation. Plots of $\langle \kappa^2 \rangle$ vs. R (Fig. 8) can quantify any potential correlation over the full range or any subrange of R .

After testing the different assumptions the simulation data can then be used to assist in the analysis of data from FRET experiments. When doing so it is helpful to consider the following 4 cases:

Case 1: both the dynamic and isotropic conditions are fulfilled. $\langle \kappa^2 \rangle$ can be set to 2/3 and R can be determined from measured FRET efficiency using the R^{-6} relationship.

Case 2: the dynamic condition is fulfilled but donor and/or acceptor molecules show restricted rotational motion and hence do not satisfy the isotropic condition. $\kappa_{ij}^2(t)$ can be replaced by $\langle \kappa^2 \rangle$ which is calculated from the simulation data but is not necessarily equal to 2/3. It is also possible to calculate the % error in R that is introduced by assuming $\langle \kappa^2 \rangle = 2/3$ by considering the range of κ_{ij}^2 values.

Case 3: the dynamic condition is not fulfilled and the static orientational averaging regime applies. $\kappa_i^2(t)$ has to be used to calculate FRET efficiency. The E vs. R relationship is likely to deviate from the conventional one as shown in Fig. 10.

Case 4: κ^2 and R are correlated. The use of $\langle \kappa^2 \rangle$ is not valid even if the dynamic condition is fulfilled. $\langle \kappa^2 \rangle$ might be different for each fluorophore separation and a system-specific E vs. R relationship needs to be derived using $\langle \kappa^2 \rangle$ for the appropriate ranges of R values. The different $\langle \kappa^2 \rangle$ values can be obtained from κ^2 vs. R plots as shown in Fig. 8.

Case 2 is a likely scenario for systems where the dyes are attached to a large or rigid host. Previous simulation studies^{13,15,17} showed that the mobility of fluorophores is clearly influenced by their environment. The interactions between the dyes and the host or other molecules close by can cause the dyes to exhibit preferred orientations and cause restricted rotational freedom.

If the system fits within the static orientation averaging regime the simulation data are of especially great value. As pointed out earlier, debates around the validity of FRET for distance measurements often emphasise that FRET efficiency should not be used to calculate R under static conditions. This is a direct consequence of the inability to determine a system wide value for $\langle \kappa^2 \rangle$ that relates E and R . But using simulation data it may be possible to derive a system-specific relationship between E and R to calculate R from experimentally observed FRET efficiencies, without the need for knowing $\langle \kappa^2 \rangle$ (Fig. 10). This approach requires the simulation to sample a sufficiently large range of R . This might not be the case if the host is a rigid molecule or in a stable conformation.

5. Conclusions

In this study we presented MD simulations of a simple model system consisting of independent fluorophores in solution where it can be expected that the dynamic and isotropic conditions are met. We used such a simple model system to investigate whether we can reproduce the expected behaviour and predict the value of κ^2 and FRET efficiency. We further investigated the assumptions commonly made in FRET experiments. By simulating multiple donors and acceptors we were able to show that the fluorophores are freely rotating. The model successfully reproduced the theoretical E vs. R relationship for both the static and dynamic case and we further demonstrated a protocol that can be used to test the assumptions commonly used in FRET experiments. Based on this analysis the simulation data can be used to calculate the numerical value and uncertainty of $\langle \kappa^2 \rangle$ and, if required or possible, a system specific E vs. R relationship can be derived.

As a concluding remark it is worthwhile to reflect on the limitations and requirements of using MD simulations to aid in the understanding and interpretation of FRET experiments and how these depend on the system under investigation. In this study we employed a simple model system but ultimately the aim is to use MD simulations to investigate more complex systems that complement real FRET experiments. To derive accurate average properties from the simulation, sufficient sampling of both rotational and translational motion of the

dyes is crucial. Our results show that even in our simple situation, simulations lasting longer than 200 ns would be required to accurately sample the fluorophore separations and κ^2 if only a single DA pair had been included. This presents a warning to those conducting simulations in more complicated situations where it is unlikely that so many DA pairs could be included in one simulation. Although attaching the dyes to a host will likely reduce their translational freedom, the time required to sample the possible fluorophore separations is not necessarily reduced as the host molecule itself needs to visit all possible conformations. Hence the sampling requirement of the translational motion is simply shifted from the motion of the dye to the conformations of the host molecule. In addition, the rotational motion can be significantly reduced by the host environment and any slower re-orientation would increase the sampling time.¹⁵ Hence it is worthwhile to focus future efforts on investigating how sampling in FRET simulations can be improved.

Acknowledgements

This work was supported by funding from the Australian Research Council, an award under the Merit Allocation Scheme on the NCI National Facility at the ANU and computer time from iVEC. ED likes to thank the Australian Federation of University Women for the Beryl Henderson Memorial Grant and the University of Western Australia for the Jean Rogerson Postgraduate Scholarship.

References

- 1 T. Förster, *Ann. Phys. (Leipzig)*, 1948, **2**, 55–75.
- 2 L. Stryer and R. Haugland, *Proc. Natl. Acad. Sci. U. S. A.*, 1967, **58**, 719–726.
- 3 P. Selvin, *Nat. Struct. Biol.*, 2000, **7**, 730–734.
- 4 R. Clegg, *Methods Enzymol.*, 1992, **211**, 353–388.
- 5 E. Haas, *ChemPhysChem*, 2005, **6**, 858–870.
- 6 T. Heyduk, *Curr. Opin. Biotechnol.*, 2002, **13**, 292–296.
- 7 P. Selvin, *Biophys. J.*, 2003, **84**, 1–2.
- 8 R. Roy, S. Hohng and T. Ha, *Nat. Methods*, 2008, **5**, 507–516.
- 9 B. Schuler, E. Lipman, P. Steinbach, M. Kumke and W. Eaton, *Proc. Natl. Acad. Sci. U. S. A.*, 2005, **102**, 2754–2759.
- 10 R. Best, K. Merchant, I. Gopich, B. Schuler, A. Bax and W. Eaton, *Proc. Natl. Acad. Sci. U. S. A.*, 2007, **104**, 18964–18969.
- 11 A. Munoz-Losa, C. Curutchet, B. Krueger, L. Hartsell and B. Mennucci, *Biophys. J.*, 2009, **96**, 4779–4788.
- 12 E. Dolgikh, W. Ortiz, S. Kim, B. Krueger, J. Krause and A. Roitberg, *J. Phys. Chem. A*, 2009, **113**, 4639–4646.
- 13 L. Allen and E. Paci, *J. Chem. Phys.*, 2009, **131**, 65101–65107.
- 14 D. VanBeek, M. Zwier, J. Shorb and B. Krueger, *Biophys. J.*, 2007, **92**, 4168–4178.
- 15 B. Corry and D. Jayatilaka, *Biophys. J.*, 2008, **95**, 2711–2721.
- 16 R. Dale and J. Eisinger, *Proc. Natl. Acad. Sci. U. S. A.*, 1976, **73**, 271–273.
- 17 G. Schroder, U. Alexiev and H. Grubmuller, *Biophys. J.*, 2005, **89**, 3757–3770.
- 18 B. Corry, D. Jayatilaka, B. Martinac and P. Rigby, *Biophys. J.*, 2006, **91**, 1032–1045.
- 19 R. Dale and J. Eisinger, *Biopolymers*, 1974, **13**, 1573–1605.
- 20 R. Dale, J. Eisinger and W. Blumberg, *Biophys. J.*, 1979, **26**, 161–193.
- 21 C. DosRemedios and P. Moens, *J. Struct. Biol.*, 1995, **115**, 175–185.
- 22 B. Van Der Meer, G. Coker and S. Chen, *Resonance Energy Transfer: Theory and Data*, VCH, 1994.

-
- 23 V. Ivanov, M. Li and K. Mizuuchi, *Biophys. J.*, 2009, **97**, 922–929.
- 24 J. Phillips, R. Braun, W. Wang, J. Gumbart, E. Tajkhorshid, E. Villa, C. Chipot, R. Skeel, L. Kale and K. Schulten, *J. Comput. Chem.*, 2005, **26**, 1781–1802.
- 25 A. MacKerell, D. Bashford, M. Bellott, R. Dunbrack, J. Evanseck, M. Field, S. Fischer, J. Gao, H. Guo, S. Ha, D. Joseph-McCarthy, L. Kuchnir, K. Kuczera, F. Lau, C. Mattos, S. Michnick, T. Ngo, D. Nguyen, B. Prodhom, W. Reiher, B. Roux, M. Schlenkrich, J. Smith, R. Stote, J. Straub, M. Watanabe, J. Wiorkiewicz-Kuczera, D. Yin and M. Karplus, *J. Phys. Chem. B*, 1998, **102**, 3586–3616.
- 26 S. Feller and A. MacKerell, *J. Phys. Chem. B*, 2000, **104**, 7510–7515.
- 27 *Molecular Probes: The Handbook - R0 values for some Alexa Fluor dyes - Table 1.6*, 2010, <http://www.invitrogen.com/site/us/en/home/References/Molecular-Probes-The-Handbook/tables/R0-values-for-some-Alexa-Fluor-dyes.html>.
- 28 J. Lakowicz, *Principles of Fluorescence Spectroscopy*, Kluwer Academic/Plenum Publisher, New York, 1999, 2nd edn.